

*Pyroxene and magnetite phenocrysts from the Taupo
quaternary rhyolitic pumice deposits, New Zealand*

By A. EWART

New Zealand Geological Survey, Lower Hutt

[Taken as read 8 June 1967]

Summary. Chemical data are presented for four hypersthènes and one coexisting hypersthène-augite pair, and chemical, X-ray, and thermomagnetic data presented for five titaniferous magnetites, all from various horizons of the Taupo pumice sequence. These phenocrysts are regarded as primary crystallization products, and not of xenocrystic origin. The hypersthènes range from $\text{Mg}_{46.4}\text{Fe}_{51.4}\text{Ca}_{2.2}$ to $\text{Mg}_{65.7}\text{Fe}_{31.2}\text{Ca}_{3.1}$; the augite composition is $\text{Mg}_{48.5}\text{Fe}_{12.3}\text{Ca}_{39.2}$. The occurrence of such magnesian pyroxenes may be explained by the early separation of titaniferous magnetite, although it is also possible that the initial iron ratios of the liquids were already sufficiently low to precipitate these pyroxenes.

The magnetites exhibit varying stages of oxidation. Data on the least oxidized specimens indicate they were initially magnetite-ulvöspinel solid solutions, with 40 to 50% (mol.) solid solution ulvöspinel. Subsequent oxidation has modified their compositions; there is some evidence that this could have occurred during normal weathering processes.

THIS paper presents chemical data on the pyroxenes and magnetites of the Taupo pumice deposits, supplementing the previously published analytical data on the glasses and plagioclases (Ewart, 1963) in which data on the pyroxenes were inferred from optics only.

The pumice deposits have been divided into 26 distinct horizons (members 1 (youngest) to 26), and these grouped into 10 eruptive episodes, i.e., during the course of one eruptive episode, several distinct horizons were generally deposited. Radiocarbon dates put an age *c.* 130 A.D. on the youngest deposits; the oldest are *c.* 10 000 years. With the exception of members 1 and 2, all the deposits are of air-fall origin. Member 1 is believed to be of glowing avalanche origin; member 2 may be of phreatic or glowing avalanche origin. The centres of eruption are believed to lie in the area around the north-eastern corner of the Lake Taupo. Further details on the field relations of these deposits are given by Baumgart (1954) and Healy (1964).

This study is based on the samples described in previous work (Ewart, 1963).

Chemistry of the pumice deposits. The calculated average composition

of the pumices, based on the average composition of eight analysed glasses (Ewart, 1963), together with modal data and analysed phenocryst data, is: SiO_2 70.60, Al_2O_3 13.23, Fe_2O_3 0.75, FeO 1.39, MgO 0.30, CaO 1.56, Na_2O 4.58, K_2O 2.86, TiO_2 0.20, P_2O_5 0.04, MnO 0.11, $\text{H}_2\text{O} + 3.26$, $\text{H}_2\text{O} - 0.70$, sum 99.58%. In view of the relatively small chemical variations found within the glasses and their low modal phenocryst contents (table I), this calculated composition is considered to provide a close approximation to the average chemistry of the pumices. The

TABLE I. Modal analyses of pumices (recalculated to 100% solid constituents). Numbers refer to their stratigraphic position within the pumice sequence

Member no.	2	3	15	19	25	Average mode of Taupo pumices*
Glass	96.3	95.7	98.9	95.3	93.6	95.7
Phenocrysts						
Plagioclase	2.9	3.6	1.1	3.5	5.5	3.7
Quartz	—	—	—	—	—	tr.
Hypersthene	0.7	0.5	< 0.1	0.8	0.7	0.4
Augite	—	—	—	0.2	—	< 0.1
Magnetite	0.1	0.2	< 0.1	0.2	0.2	0.2
Hypersthene/Augite ratio†	12	—	> 20	2	10	n.d.

* Determined from data in table 2, Ewart 1963 (p. 401).

† Determined by frequency counts on heavy mineral fractions.

composition is rhyolitic; a notable feature, common to the acidic volcanic rocks of the Taupo Volcanic Zone, is the relatively high $\text{Na}_2\text{O}/\text{K}_2\text{O}$ ratio.

Mineralogy. The phenocrysts comprise plagioclase (intermediate to basic andesine), hypersthene, augite, magnetite, and minor ilmenite (comprising less than a fifth of the total opaque minerals). The total crystal contents of the pumices are very low, and there is little variation between the various members (table I). Quartz is very rare. There are, however, small but probably significant variations in the hypersthene/augite ratio (table I); In general, this ratio is lower in the older deposits (e.g. 19 and 25). It was also noted (Ewart, 1963) that the ratio tends to decrease towards the end of each eruptive episode.

From the study of the rhyolitic lavas of the Taupo Volcanic Zone (Ewart, 1967), it has been concluded that the hypersthene or hypersthene-augite ferromagnesian assemblage occurred in lavas with low crystal contents, and little or no quartz; hornblende and biotite tend to appear in rocks with progressively higher crystal contents, and presumed

falling liquidus temperatures. The occurrence of hypersthene and augite only in the low-crystal-content Taupo pumices is therefore in accordance with these results.

Pyroxenes

All samples were crushed to -230 mesh, and washed. Initial purification was done by centrifuging the samples in Clerici solution. Final purification was achieved on the Franz isodynamic separator—this was found to be the only method that completely separated augite and hypersthene and also removed hypersthene grains containing small magnetite inclusions. Apatite inclusions could not be removed, and all the P_2O_5 in the chemical analyses (table II) is assumed to represent apatite (the appropriate CaO being allotted in the calculation of the formulae). Unfortunately, augite, in sufficient quantity for chemical analysis, could only be separated from member 19.

Hypersthene phenocrysts typically occur as fresh, thick, euhedral prismatic crystals, mostly averaging between 0.1 to 0.4 mm in length. Inclusions are always present, comprising euhedral magnetite (common), needle-like apatite and zircon (the latter relatively uncommon), and blebs of glass. No exsolution has been noted optically, and zoning appears to be uncommon, although the range of refractive indices (table II) seems to indicate limited compositional variation within each sample.

Augite typically occurs as pale green, short, thick prismatic crystals, usually slightly smaller on average than the coexisting hypersthene. Inclusions of magnetite, apatite, and glass have been noted, but they tend to occur less abundantly and are smaller than in the hypersthene.

The coexisting pyroxenes normally occur as separate crystals, but occasionally are found in contact. There does not appear to be any reaction relationship in such cases. Each pyroxene has been observed to form partial envelopes around the other.

Chemistry. The most significant point is the confirmation of the magnesian nature of the pyroxenes (table II), which are closely comparable to those described by Carmichael (1963). Some discrepancy, however, exists between the optically and chemically determined compositions. In particular, the pair from Member 19 are appreciably more magnesium-rich than previously suggested (Ewart, 1963). The following points, which may be significant, arise from the chemical data: The hypersthene from the two older members are more magnesium-rich than those from the younger members; these two older members also have a relatively high augite content. There is a progressive decrease of TiO_2 in the hypersthene from oldest to youngest; Verhoogen (1962)

has suggested that the entry of titanium into pyroxenes is determined by temperatures. MnO closely follows FeO in the hypersthene. With the exception of the pyroxenes from Member 19, both Ti and Fe''' appear

TABLE II. Chemical analyses and formulae of pyroxene phenocrysts

	Member 2 Hyper- sthene*	Member 3 Hyper- sthene†	Member 15 Hyper- sthene*	Member 19 Hyper- sthene* Augite*	Member 25 Hyper- sthene*	
SiO ₂	48.7	48.0	50.1	52.3	51.5	
TiO ₂	< 0.05	0.07	0.25	0.28	0.35	
Al ₂ O ₃	1.2	1.5	0.4	1.9	0.15	
Fe ₂ O ₃	1.85	0.80	1.85	0.2	3.45	
FeO	26.2	26.5	28.0	18.8	22.15	
MnO	1.85	1.8	2.05	0.46	0.90	
MgO	18.05	18.7	16.05	23.0	19.9	
CaO	1.90	2.7	1.50	1.6	1.3	
Na ₂ O	0.10	0.20	0.08	0.10	0.08	
K ₂ O	0.05	—	0.06	—	0.02	
P ₂ O ₅	0.20	0.26	0.30	0.07	0.18	
Total	100.10	100.53	98.64	98.71	99.98	
α min	1.706	1.706	1.710	1.695	1.707	
β	n.d.	n.d.	n.d.	n.d.	n.d.	
γ max	1.721	1.722	1.727	1.715	1.725	
2 V	n.d.	56°(-)	50°-52°(-)	55°-60°(-)	46°(+)	54°-56°(-)
Ca/(Ca+Mg+Fe)	3.3 %	4.6	2.2	3.1	39.2	2.2
Mg/(Ca+Mg+Fe)	50.3 %	51.0	46.4	65.7	48.5	56.3
Fe/(Ca+Mg+Fe)	46.4 %	44.4	51.4	31.2	12.3	41.5
Mg (determined from optics)	54 %	54-55	48-51	59-64	42	51-54

Formulae of the analysed pyroxenes (on the basis of six oxygens). All P₂O₅ assumed to go into apatite.

Z	Si	1.899	1.871	1.956	1.953	1.898	1.958
	Al	0.055	0.069	0.018	0.047	0.102	0.007
	Ti	—	0.002	0.007	—	—	0.010
	Fe ³⁺	0.046	0.023	0.019	—	—	0.025
WXY	Al	—	—	—	0.036	0.016	—
	Ti	—	—	—	0.008	0.010	—
	Fe ³⁺	0.008	—	0.035	0.006	0.059	0.074
	Fe ²⁺	0.852	0.864	0.914	0.587	0.179	0.704
	Mn	0.061	0.059	0.068	0.015	0.004	0.029
	Mg	1.049	1.086	0.933	1.279	0.954	1.127
	Ca	0.069	0.099	0.046	0.060	0.771	0.043
	Na	0.007	0.015	0.006	0.007	0.021	0.006
	K	0.002	—	0.003	—	—	0.001
	Z	2.000	1.965	2.000	2.000	2.000	2.000
WXY	2.048	2.123	2.005	1.998	2.004	1.984	

* Analyst: J. A. Ritchie } Chemistry Division, New Zealand Dept. Sci. Indust. Res.,
 † Analyst: P. Curtis } Gracefield.

to be required to fill the Z position (assumed to equal two atoms per formula); Fe₂O₃ does not appear to be abnormally high in the original mineral analyses. The Ca of the hypersthene appears to be near (or even slightly above in Members 2 and 3) the expected maximum of Ca₃ suggested by Deer, Howie, and Zussman (1963). The augite from Member 19 appears more enriched in Mg relative to its coexisting hypersthene than is normal (cf. tie lines from Carmichael (1963) plotted

in fig. 1 for comparison); this is confirmed by the calculated distribution coefficient, $K_D = 0.41$ (after Kretz, 1961), which is very low; even assuming that oxidation of the ferrous iron has occurred and recalculating K_D including Fe^{3+} , a value of 0.54 is obtained, which is still very low for pyroxene pairs of igneous origin; other elements, however, show normal distribution between the coexisting pyroxenes and there are no textural reasons to suppose that the two pyroxenes were not in equilibrium.

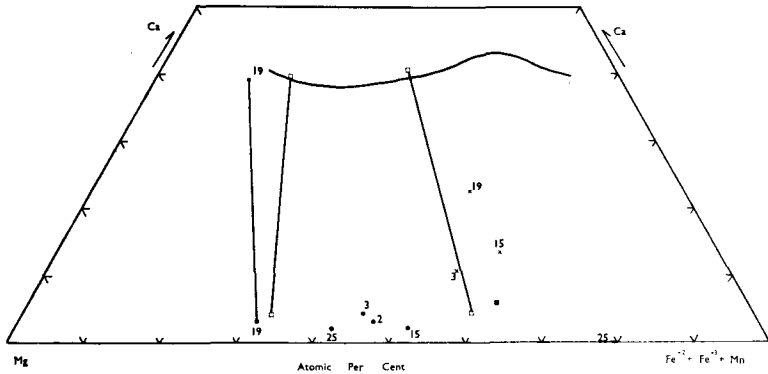


FIG. 1. Crystallization trend of calcium-poor and calcium-rich pyroxenes from selected members of the Taupo pumice sequence. Numbers refer to stratigraphic positions of deposits from which pyroxenes were separated. Also shown are the normative Wo, En, and Fs components of the coexisting glasses and the average total composition of pumices. Two additional coexisting pyroxene pairs and the pyroxene trend of the British and Icelandic Tertiary acid glasses are from Carmichael (1960). ● hypersthene, ○ augite described in this paper. □ two pyroxene pairs analysed by Carmichael (1960). ×, ■ Wo, En, Fs components of glasses and average total pumice respectively.

Discussion. The magnesian-rich nature of the pyroxenes would usually be considered anomalous in rhyolitic rocks. However, the compositions are similar to those described by Carmichael (1963), and are also typical of the pyroxenes found in other rhyolitic rocks of the Taupo Volcanic Zone (Ewart, 1965, 1966). Carmichael (1963) has attributed the magnesium-rich nature to the early separation of magnetite, which causes depletion of iron in an already iron-poor melt. This explanation could certainly be applied to the present case, and it is possible that variations in the number of magnetite inclusions in the crystals could result in variations in bulk composition between crystals.

In fig. 1, the normative Di, En, and Fs components of the glasses coexisting with the pyroxene are plotted, together with the average total

composition. From the relative positions of the glasses and total composition, there seems little difference in Mg:Fe ratios, and this suggests that in fact the acid liquids were already sufficiently low in Fe relative to Mg to precipitate Mg-rich pyroxenes, even without the prior separation of magnetite.

Additional factors, however, appear to influence the variations in composition of the pyroxenes between the various members. For example, it was shown (Ewart, 1963) that the more Ca-rich plagioclase phenocrysts occur in deposits containing the most Mg-rich pyroxenes (and also lowest hypersthene/augite ratios). This suggests higher liquidus temperatures during their crystallization.

The apparently anomalous Mg-Fe²⁺ distribution between the co-existing pyroxenes from Member 19 requires some explanation, and raises the question of whether the 'ideal' partition of elements would necessarily occur between coexisting minerals that are present only in very small quantities within a magma. As previously noted, both Mg and Fe contents are very low in the pumices, and local compositional inhomogeneities in the original magma could produce significant variations in the Mg:Fe²⁺ ratios. Such variations could also be produced by magnetite crystallization, or local differences in P_{O_2} . An additional factor affecting element partition in these circumstances would occur if one of the pyroxenes either began or ceased to be precipitated before the other, again resulting in different Mg:Fe²⁺ ratios of the magma during the crystallization of each pyroxene. The above discussion seems to receive some support from the fact that the hypersthene compositions from the various pumice deposits do vary appreciably, in spite of only very minor differences in the compositions of the glasses (Ewart, 1963).

Magnetites

Initial separations were attained, after crushing to -230 mesh and washing, by repeated centrifuging in warm Clerici solution. Separations were then continued by passing the samples through a Franz isodynamic separator (with a current of 0.05 amp). Only the material actually adhering to the magnet was retained. In spite of this, up to 5% silicate impurities remained, comprising volcanic glass and hypersthene. As the compositions of these impurities were known, corrections were made in the recalculated analyses (table III). Apatite inclusions were also present, while very rare grains of pyrite were noted.

As previously noted, euhedral magnetite crystals are ubiquitous inclusions in the pyroxenes. Discrete microphenocrysts also occur

distributed through the pumices, generally ranging in size from 0.08 to 0.2 mm. The following notes are based on reflected light examination of polished mounts, under $\times 1050$ magnification: In each sample, the majority of grains consist of an optically homogeneous magnetite phase.

TABLE III. Partial chemical analyses, unit cell data, and potential normative composition of magnetite phenocrysts. Analyst: J. A. Ritchie

	Member 2	Member 3	Member 15	Member 19	Member 25
SiO ₂	3.2	2.8	3.0	1.7	2.5
TiO ₂	15.2	12.4	14.0	9.1	14.4
Al ₂ O ₃	2.1	2.1	1.7	3.1	2.1
Fe ₂ O ₃	40.1	41.2	39.5	51.8	44.3
FeO	35.2	38.3	38.7	30.4	34.2
MnO	0.76	0.74	0.73	0.39	0.48
MgO	0.8	0.5	0.5	1.8	0.2
Total	97.36	98.04	98.13	98.29	98.18
<i>a</i>	8.434 ± 0.002 Å	8.436 ± 0.302	8.442 ± 0.001	8.437 ± 0.003	8.439 ± 0.002
<i>Normative compositions, wt %, according to method of Vincent et al., 1957:</i>					
<i>Magnetite, etc.</i>					
Fe ₂ O ₄	56.7	58.6	56.0	64.8	63.2
FeAl ₂ O ₄	3.3	3.1	2.3	4.9	3.1
MnFe ₂ O ₄	1.4	1.2	1.2	0.9	0.9
MnAl ₂ O ₄	0.2	0.2	0.2	—	—
MgFe ₂ O ₄	—	—	—	3.6	—
MgAl ₂ O ₄	—	—	—	0.3	—
<i>Ulvöspinel, etc.</i>					
Fe ₂ TiO ₄	4.2	21.7	22.1	—	0.7
Mn ₂ TiO ₄	0.2	0.4	0.4	—	—
<i>Ilmenite, etc.</i>					
FeTiO ₃	25.2	8.3	11.1	16.1	26.4
MnTiO ₃	0.6	0.2	0.2	0.3	0.5
MgTiO ₃	—	—	—	0.7	—
Excess Fe ₂ O ₃	—	—	—	3.5	—
Silicate	5.5	4.4	4.7	3.1	3.4
Σ Magnetite	61.6	63.1	59.7	74.5	67.2
Σ Ulvöspinel	4.4	22.1	22.5	—	0.7
Σ Ilmenite	25.8	8.5	11.3	17.1	26.9
<i>Molecular Proportions:</i>					
MO	51.1	55.2	55.1	48.7	50.2
R ₂ O ₃	28.7	28.7	26.9	38.8	30.9
TO ₂	20.2	16.1	18.0	12.5	18.9

However, the remaining grains exhibit some form of 'exsolution-type' or 'replacement-type' texture resulting from oxidation. Four types of 'exsolution' texture were observed (cf. Buddington and Lindsley, 1964, p. 322): relatively coarse, but regular lamellae of optically homogeneous titanhematite phase cutting the magnetite phase (Fig. 2); the same, but with additional very fine lamellae of a dark aluminous spinel exsolved from the magnetite phase; grains consisting almost entirely of the homogeneous ilmenite-hematite phase, with a few residual lamellae of the magnetite phase (these are the extreme end-products of the first

type, the residual magnetite phase being poor in Ti and enriched in Al, Mg, and Mn (Wright and Lovering, 1965)); and extremely fine intersecting lamellae of ilmenite (as evidenced by their pinkish colour and similar reflectivity to the magnetite) within the magnetite phase.

Two distinct 'replacement' textures were observed: marginal alteration (martitisation) of the magnetite phase to a homogeneous ilmenite-hematite, the latter phase also forming anastomosing veinlets extending

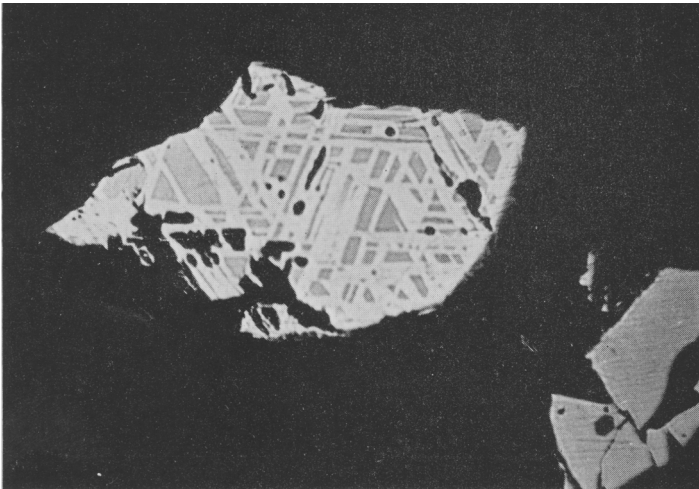


FIG. 2. Titanhematite lamellae (white to pale grey) within magnetite phase (medium grey). Part of a homogeneous titaniferous grain is visible in lower right corner of photograph. Member 19. $\times 1200$. Photo: S. N. Beatus.

into the magnetite; and grains showing alteration to ilmenite-hematite and associated with a red transparent mineral, assumed to be goethite.

A striking feature of these textural types is their similarity to the New Zealand ironsand deposits described by Wright (1964). An approximate estimate of grains showing textural inhomogeneities (based on counts of 400–500 grains) gave:

Member	2	3	15	19	25
Homogeneous	33	94	93	67	76
'Exsolution' grains	6	2	3	19	10
'Replacement' grains	11	4	4	14	14

This table shows that the two oldest magnetites (19 and 25) contain the highest percentage of oxidized grains. A further feature shown is the

sympathetic increase of both 'exsolution' and 'replacement-type' grains with increasing oxidation. The possible implications of this feature will be discussed later. The degree of oxidation of the magnetites, as determined by the percentage of homogeneous grains, agrees well with the conclusions reached from the chemical data.

X-ray data. Cell dimensions¹ are given in table III. In addition to the magnetite reflections, the main hematite and ilmenite reflections were also identified:

Member	2	15	19	25
c. 2.74 Å (= ilmenite)	weak	v. weak	v. weak	weak
c. 2.69 Å (= hematite)	weak	v. weak	moderate	weak

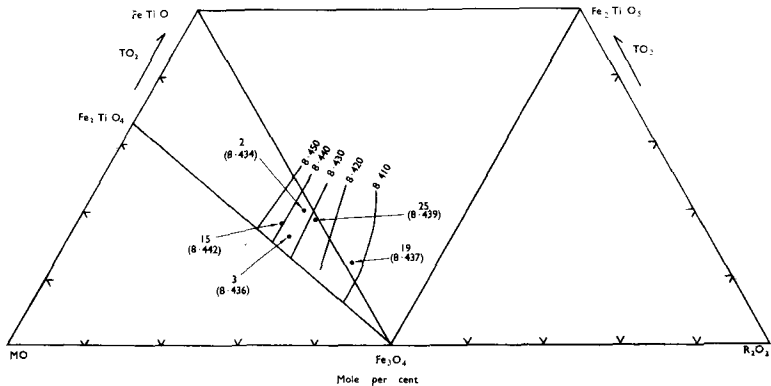


FIG. 3. Compositions of titaniferous magnetite phenocrysts plotted in system $MO-R_2O_3-TO_2$. Superimposed are the lattice parameter contours (for one-phase spinels from volcanic rocks) after Akimoto, Katsura, and Yoshida (1957). Numbers (arrowed to the plotted points) refer to stratigraphic positions of deposits (as in fig. 1) and the determined cell dimensions (in brackets; see table III).

Oxidation will account for the presence of both ilmenite and hematite. The magnetite reflections were mostly relatively sharp (with the exception of the Member 19 sample); as the magnetites analysed were derived both from inclusions in the pyroxenes and from discrete microphenocrysts, it is assumed that no significant compositional differences exist between the two types of occurrence.

Chemistry. Analyses and potential normative compositions of the separated titanomagnetites are presented in table III and plotted in fig. 3 in terms of $MO-R_2O_3-TO_2$. As expected, samples from Members

¹ Determinations made from powder photographs taken in a Philips 111.43 mm camera using Fe- $K\alpha$ radiation.

2, 3, and 15, with least proportion of oxidized grains, are richer in ulvöspinel, while that for Member 19, the most oxidized, shows excess normative Fe_2O_3 .

MnO shows some significant variation between the samples—it is notably lower in the magnetites coexisting with the most Mg-rich pyroxenes (19 and 25). MgO was reported in the original analyses from all five samples; with the exception of the magnetite from Member 19, however, the MgO was found to be present in the silicate impurities. In 19, even after correction for the silicate impurities, considerable MgO remained and is assumed to be in solid solution in the magnetite. This may be significant, as the most Mg-rich pyroxenes coexist with this magnetite.

Magnetic study. Curie point measurements were carried out by Dr. T. Hatherton and Mr. A. E. Leopard at the Geophysics Division, N.Z. Department of Scientific and Industrial Research, using a converted chemical balance as the basis for the apparatus. The specimens (0.2 gm) were sealed *in vacuo* in small pyrex tubes. Balancing was performed by adding and subtracting small weights.

The results are presented in fig. 4, in order of increasing oxidation, as deduced from the chemistry and mineralogy of the samples. The two least oxidized specimens (3 and 15) exhibit relatively sharp Curie temperatures between 220 and 300° C, which are interpreted as due to the titaniferous magnetite. Using the data of Nagata and Akimoto (1961, p. 82), these Curie temperatures indicate 45 to 51 mol. % solid solution ulvöspinel in specimen 3 and 50 to 55 % in specimen 15.

With progressive oxidation (2, 25, 19), the curves show a progressive flattening of slope and migration to higher temperatures, i.e. there is an increasingly widening range of Curie temperatures. This can be interpreted in two ways.

The first explanation (following Wright and Lovering, 1965, pp. 618–20) rests on the fact that when oxidation commences much of the Ti migrates into the rhombohedral lamellae; this results in the rise of the Curie point of the cubic phase to about 500° C; the diluent effect of Al, Mg, and Mn remaining in the cubic phase accounts for the lowering of the Curie temperature below the expected maximum of 580° C. Increasing oxidation results in the cubic phase becoming strongly enriched in Mg, Al, and Mn, causing a further lowering of the Curie point. The presence of grains in various stages of oxidation thus results in a smoothing of the slope of the thermomagnetic curve from the lower to the higher Curie temperatures.

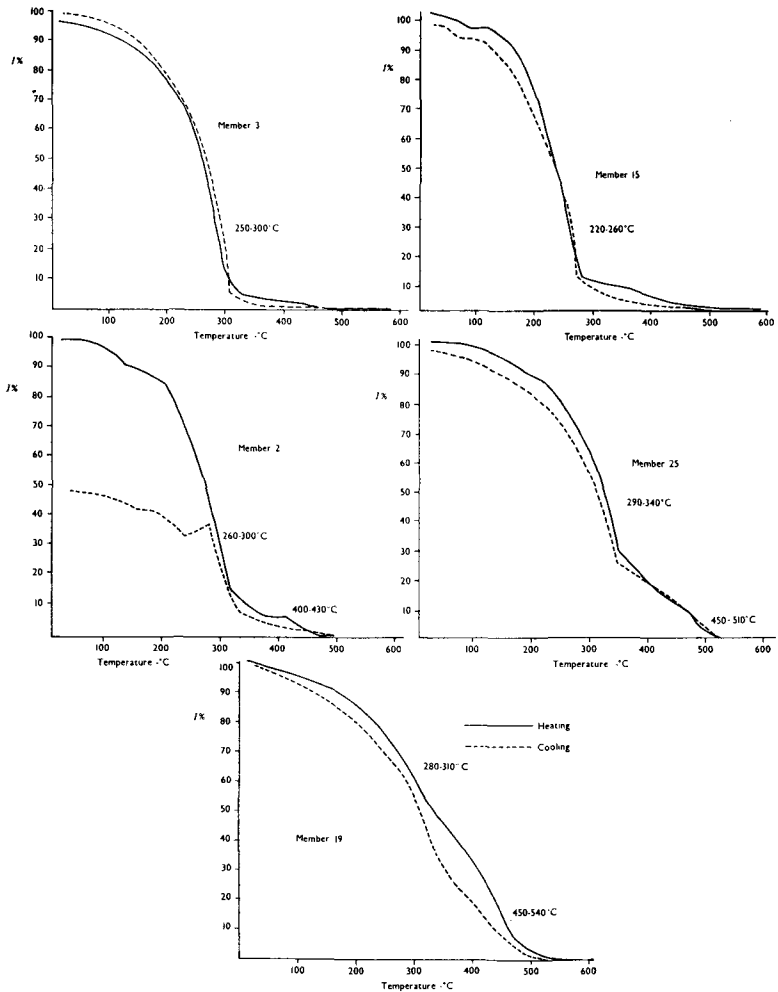


FIG. 4. Thermomagnetic curves for the five analysed magnetite samples (table III). The curves have been arranged in order of increasing oxidation (Members 3, 15, 2, 25, and 19 respectively) as determined from the chemical and mineralogical data.

The second explanation simply involves the progressive production of titanhematite. Pure hematite has a Curie point of 680°C , while the higher temperature range of Curie points in fig. 4 lies between about 450 to 540°C . This lowering of the temperature can be attributed to the presence of titanium, equivalent to approximately 20% (mol.)

solid solution ilmenite (Nagata and Akimoto, 1961, p. 108), which agrees approximately with the data for the fully oxidized grains presented by Wright and Lovering (1965).

In fact, both mechanisms may be operative in the modification of the Curie temperatures during oxidation. It is of interest to note that the thermomagnetic curve of the most oxidized sample (19) is practically identical to those shown by Wright (1964, p. 434) from the New Zealand titaniferous beach sands.

Finally, the presence of small amounts of ilmenite may account for the small changes of slopes occurring at 80–120° C in the thermomagnetic curves of samples 15 and 2 (fig. 4).

Discussion. Using the data of Vincent *et al.* (1957), the range of cell dimensions given in table III indicate between 38 and 47% solid solution ulvöspinel in the magnetites. The mol. per cent solid solution ulvöspinel in the magnetites from Members 3 and 15, estimated from these cell sizes, is 41% and 47% respectively. In fig. 3, the analyses of those two magnetites plot fairly close to the ulvöspinel-magnetite join, and an estimate of their content of ulvöspinel has been made by projecting (parallel to the theoretical oxidation lines) the compositions on to the join. The estimates made by this method give 47% (3) and 52% (15). The agreement between the estimates by the two methods is relatively close, and indicates that the magnetites were initially magnetite-ulvöspinel solid solutions. The cell dimensions of the three least oxidized samples (3, 15, 2) also show good agreement with their bulk chemical compositions, as judged from the lattice parameter contours (for one phase spinels) superimposed on fig. 3 (after Akimoto, Katsura, and Yoshida, 1957). The cell sizes of all five magnetites show relatively little variation, and this is considered to reflect initially similar compositions.

From fig. 3, some discrepancy is evident between cell dimensions and chemistry of the two most oxidized samples (25 and, especially, 19). The TiO₂ content of 19 (table III) is very much lower than the other samples. This sample is the most oxidized, and it is suggested that prior to the mineral separation procedures, there was in fact a larger proportion of crystals showing inhomogeneities than is shown above. Subsequent crushing and separation techniques have freed and removed some of these titanhematite products. Wright and Lovering (1965) have shown that Ti rapidly builds up in the rhombohedral phase during oxidation; thus, preferential removal of this phase during separation can result in the lowering of TiO₂ in the final bulk chemical analysis of the magnetite sample. The powder photograph of this sample (19)

showed somewhat diffuse and weak reflections. It is suggested that the measured cell dimension represents that of the remaining unoxidized grains, i.e. it should approximate to the original cell dimension prior to oxidation.

The oxidation of the magnetites to ilmenite-hematite phases is thus interpreted (cf. Wright, 1964) as a post-crystallization process, but at what stage is uncertain—whether during eruption or after eruption or both. It is relevant to note that the two most oxidized magnetites (of the five analysed) are from the two oldest and most weathered members. Furthermore, Member 19 has a well-developed soil on it (Healy, 1964) and this horizon contains the most oxidized specimen (table III and fig. 3). As noted previously, the magnetites from 3 and 15 are the least oxidized, and that from 15 (the older) appears the slightly more oxidized of the two (table III). The sample from Member 2, however, is apparently an exception to this possible weathering-oxidation trend. A possible explanation is that this deposit was of glowing avalanche or even phreatic origin and that oxidation took place during the eruptive process.

It is postulated from this evidence presented that the oxidation of these magnetites is a post-eruptive weathering phenomenon. This implies that the 'exsolution-type' textures were produced under normal temperatures and pressures, as grains showing these textures were shown to increase in number with oxidation. Initially, it was inferred (cf. Wright, 1964) that such low-temperature oxidation would occur by the increasing marginal alteration of magnetite grains (martitisation), and that the 'exsolution-type' textures were produced during the cooling phase. It must be pointed out, however, that other factors cannot be ruled out on the above evidence. For example, reheating of an earlier-deposited pumice deposit by later erupted material, or differences in heights to which the deposits were ejected, resulting in variations in the rates and amounts of cooling before deposition. These factors cannot yet be evaluated in the deposits under discussion. The amount of ionic migration involved in the formation of the lamellae would certainly seem to require reasonably elevated temperatures.

Conclusions

The magnesian pyroxenes and the magnetites are regarded as true primary crystallization products of the acidic magma, there being no textural evidence for a xenocrystic origin. For example, the range of compositions of the pyroxenes, the association of the most Mg-rich pyroxenes and Ca-rich plagioclases, the occurrence of lower Mn in the

magnetites coexisting with the most Mg-rich pyroxenes, and the association of lower hypersthene/augite ratios with more Mg-rich pyroxenes, all point against any accidental origin of these phenocrysts. Some discrepancy is apparent, however, in the Mg:Fe²⁺ ratios of the only analysed coexisting augite-hypersthene pair. It is suggested that when such coexisting pairs occur in a magma in such small amounts, they would be susceptible to anomalous Mg-Fe²⁺ partition even if only small local compositional inhomogeneities existed in the magma. Carmichael (1963) has argued that a depletion of iron will occur in a crystallizing liquid by the early separation of magnetite, resulting in the precipitation of relatively magnesian pyroxenes. There is little doubt that this mechanism has been operative in the magmas giving rise to the Taupo pumices. It is also possible, however, that a normal although limited iron enrichment subsequently took place after the eruption of the earlier deposits, as the pyroxenes within the three younger deposits (2, 3, and 15) are slightly richer in Fe and Mn. This, however, assumes that all the deposits were erupted from the same magma reservoir, which is by no means certain.

The magnetites are believed to have been initially ulvöspinel-magnetite solid solutions. Cell dimensions and thermomagnetic and chemical data on the two least oxidized specimens indicate an initial solid-solution ulvöspinel content of about 40 to 50 % for the various analysed samples. This is consistent with the results and conclusions of Carmichael (*op. cit.*), that the early-crystallizing iron-ores may contain considerable amounts of the ulvöspinel molecule, which may reflect the reduced nature of the parent acid liquids. All the magnetites show oxidation to varying degrees and there is some evidence that much of this could have occurred at low temperature, during normal weathering processes.

Acknowledgements. Grateful thanks are due to Messrs. J. A. Ritchie and P. Curtis, Chemistry Division, N.Z. D.S.I.R., for undertaking the chemical analyses, and to Dr. T. Hatherton and Mr. A. E. Leopard for making the Curie point measurements. The writer is also indebted for numerous discussions and criticisms of the manuscript to Dr. J. B. Wright, Geology Department, Otago University, and to Drs. G. A. Challis and K. R. Gill, New Zealand Geological Survey.

References

- AKIMOTO (S.), KATSURA (T.), and YOSHIDA (M.), 1957. Journ. Geomag. and Geoelect., vol. 9, pp. 165-178.
- BAUMGART (I. L.), 1954. New Zealand Journ. Sci. Tech., ser. B, vol. 35, pp. 456-467.
- BUDDINGTON (A. F.) and LINDSLEY (D. H.), 1964. Journ. Petrology, vol. 5, pp. 310-357.

- CARMICHAEL (I. S. E.), 1960. *Journ. Petrology*, vol. 1, pp. 309-336.
 — 1963. *Min. Mag.*, vol. 33, pp. 394-403.
 DEER (W. A.), HOWIE (R. A.), and ZUSSMAN (J.), 1963. *Rock forming minerals*, vol. 2, Longmans, Green, London.
 EWART (A.), 1963. *Journ. Petrology*, vol. 4, pp. 392-431.
 — 1965. *New Zealand Journ. Geol. Geophys.*, vol. 8, 611-677.
 — 1966. *Bull. Volcanologique*, vol. 29, pp. 147-172.
 — 1967. *New Zealand Journ. Geol. Geophys.*, vol. 10, pp. 182-197.
 HEALY (J.), 1964. *In New Zealand Geol. Surv. Bull.*, new ser., 73, pp. 7-42.
 KRETZ (R.), 1961. *Journ. Geol.*, vol. 69, pp. 361-387.
 NAGATA (T.) and AKIMOTO (S.), 1961. *In Rock Magnetism by Nagata (T.)* (Maruzen Company Ltd., Tokyo), pp. 75-125.
 VERHOOGEN (J.), 1962. *Amer. Journ. Sci.*, vol. 260, pp. 211-220.
 VINCENT (E. A.), WRIGHT (J. B.), CHEVALLIER (R.), and MATHIEU (S.), 1957. *Min. Mag.*, vol. 31, pp. 624-655.
 WRIGHT (J. B.), 1964. *New Zealand Journ. Geol. Geophysics*, vol. 7, pp. 424-444.
 — and LOVERING (J. F.), 1965. *Min. Mag.*, vol. 35, pp. 604-621.

[*Manuscript received 28 November 1966*]
